# Correlation effects mediated by disorders in one-dimensional channels

Vivek Kumar,[1] Yingshi Duo,[1] Patrick See,[2] Jonathan P. Griffiths,[3] David A. Ritchie,[3] Ian Farrer,[4] and Sanjeev Kumar[1,*]

[1]*Department of Electronic and Electrical Engineering, University College London, Torrington Place, London WC1E 7JE, United Kingdom*
[2]*National Physical Laboratory, Hampton Road, Teddington, Middlesex TW11 0LW, United Kingdom*
[3]*Cavendish Laboratory, University of Cambridge, J. J. Thomson Avenue, Cambridge CB3 0HE, United Kingdom*
[4]*School of Electrical & Electronic Engineering, University of Sheffield, Mappin Street, Sheffield S1 3JD, United Kingdom*

(Received 31 December 2024; accepted 18 June 2025; published 7 July 2025)

We report nonlinear transport in one-dimensional quantum wires formed in a GaAs/AlGaAs heterostructure. The two-terminal conductance characteristics were investigated under varying electron concentrations with and without a large in-plane magnetic field of 10 T. One important observation was that the 0.7-like feature was identified at higher-order subbands, specifically $\sim 1.6G_0$, $\sim 3.7G_0$, and $\sim 4.7G_0$. Additionally, our findings reveal the emergence of two conductance states appearing below $e^2/h$ under large dc bias voltage, where these states become more pronounced together with higher 0.7-like features, as electron concentration decreases, highlighting the influence of strong correlation effects in their formation. The weak Zeeman splitting in the ground state despite a large in-plane magnetic field of 10 T in low-density and weakly confined regime indicates disordered-induced correlation effects dominating the mechanism.

DOI: 10.1103/k8zm-v738

## I. INTRODUCTION

One-dimensional (1D) systems have long served as a rich platform for cultivating intricate quantum phenomena, fostering the development of new physics for decades [1,2]. In particular, semiconductor heterostructures featuring a high-mobility two-dimensional electron gas (2DEG) located at the heterostructure interface are utilized to construct a 1D quantum wire through electrostatic confinement using split-gate techniques [3]. By varying the gate voltage, electrons in the 2DEG beneath the split gates are gradually depleted, leading to the formation of a 1D constriction. When the system is cooled to low temperatures, electron transport in this narrow region enters the ballistic regime, resulting in quantized conductance plateaus at $NG_0$, where $N$ is a positive integer and $G_0 = 2e^2/h$ is a universal constant (e is the electron charge and h is the Planck's constant) [4,5]. The emergence of these plateaus occurs as the Fermi level crosses successive spin-degenerate 1D subbands when the 1D constriction width is controlled by the split gate voltage. A quasi-plateau often forms around $0.7G_0$, which is referred to as the 0.7 anomaly [6]. Although the exact origin of the 0.7 structure has not yet been established, it is essentially regarded as a correlation effect, although this effect has been produced in systems with Kondo impurities [7].

Varying the number of electrons in the 1D channel is key in tuning the degree of correlation effects or interaction between the electrons. At a low electron density, $n_{1D}$, the interaction energy ($= e^2 n_{1D}/\epsilon$) becomes prominent compared to the kinetic energy, which is typically of the order of the Fermi energy ($= \pi^2\hbar^2 n_{1D}^2/8m^*$), where $\epsilon$ is the dielectric constant of the material, $\hbar$ is the reduced Planck's constant, and $m^*$ is the effective mass of the electron. Under these conditions, electrons in the ground state rearrange in a zigzag-like structure, which splits into two rows of electrons upon further dominance of Coulomb repulsions, known as the 1D Wigner lattice [8]. The formation of such long-range ordered electron chains becomes possible when the distance between two consecutive electrons in a row, $1/n_{1D}$, called the Wigner-Seitz radius, is larger than the Bohr radius of the material [8–13]. The formation of a zigzag structure and its transformation into a Wigner lattice directly drives the emergence of fractional quantum states in the absence of a magnetic field in GaAs-based systems [1,14,15]. The weakly confined 1D channel resulted in various fractional states that were particularly pronounced at 1/2, 1/4, 1/6, and 2/5 (in units of $e^2/h$) in the absence of a magnetic field [15].

Although theoretical models predict that a small amount of disorder in the channel could pin the Wigner lattice [16–18], experimental observations of the Wigner lattice have been essentially restricted to clean quantum wires [19–21]. This raises many open questions and challenges in experiments, such as how the disorder affects the electron-electron interactions and the stability of the Wigner lattice. A particular challenge is understanding how the reorganization of electrons occurs because of the competition between electron-electron interactions, variable confinement, the Zeeman energy in the presence of a magnetic field, and the disorder potential.

This article attempts to answer some of these questions by means of conductance studies in moderately disordered 1D quantum wires using dc source-drain bias spectroscopy. A dc source-drain bias comparable to the subband spacing was

*Contact author: sanjeev.kumar@ucl.ac.uk

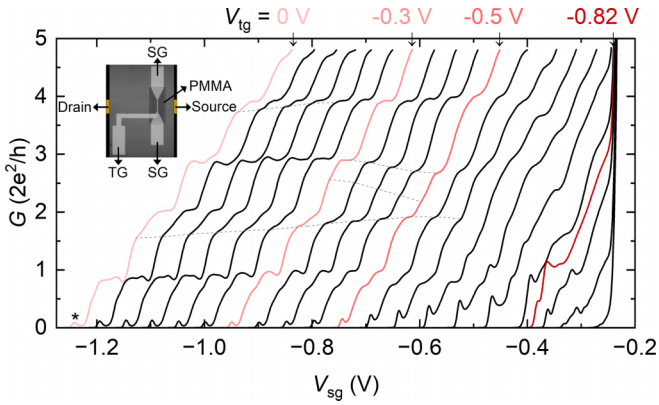


FIG. 1. Differential conductance, $G$, as a function of symmetric split gate voltage, $V_{sg}$, at various top gate voltages between $V_{tg} = 0$ V (left) and $V_{tg} = -0.95$ V (right). The inset shows an optical microscope image of a representative device. Note that the yellow blocks, representing ohmic contacts, serving as source and drain, are drawn over the optical image for clarity, and are not part of the actual optical micrograph. Conductance traces recorded at $V_{tg} = 0$, –0.3, –0.5, and –0.82 V are highlighted. The asterisk (*) indicates the resonance peak near the pinch-off. The dotted lines guide the evolution of conductance states in higher-order subbands as $V_{tg}$ varies.

used to explore nonlinear transport, which allows for probing electron correlations across different energy states. The experiments were performed under varying electron concentrations, both with and without an in-plane magnetic field. Our results show the indication of correlation effects coupled with impurity-induced influences. We also show that the system has entered the 1D Wigner regime, i.e., a zigzag of electrons, measured by nonlinear transport.

## II. EXPERIMENTAL METHODS

The devices used in this work were fabricated on a GaAs/AlGaAs heterostructure grown using molecular beam epitaxy. The 2DEG was formed at a depth of up to 90 nm beneath the surface, with a low-temperature mobility of $2.7 \times 10^6$ cm$^2$/Vs and an electron density of $1.8 \times 10^{11}$ cm$^{-2}$. A pair of split gates, each with a length of 0.8 μm and a width of 0.5 μm, and a top gate of the length of 1 μm separated by a 0.3-μm-thick insulating layer of cross-linked poly (methyl methacrylate), PMMA, were patterned by a standard lithographic technique, see inset of Fig. 1 [15,21,22]. Two-terminal differential conductance, $G = dI/dV_{sd}$, measurements were carried out using a lock-in amplifier by applying an excitation voltage of 10 μV at 73 Hz in a cryogen-free dilution refrigerator at a base temperature of 45 mK.

Conductance measurements were performed on 1D quantum wires by applying identical voltages to both split gates, creating a symmetric confinement potential. Differential conductance was recorded for different electron densities in the 1D channel controlled by the top gate voltage $V_{tg}$. Measurements in the nonlinear regime were carried out by applying a dc bias voltage between the source and drain $|V_{sd}| \leqslant 3$ mV, in addition to the ac excitation of 10 μV. For this, the $V_{sd}$ was first set to –3 mV, and the differential conductance was recorded while sweeping the split gates. This process was then repeated for each subsequent $V_{sd}$ in 0.1 mV increments up to 3 mV. The experiments were conducted at zero magnetic field and with an in-plane magnetic field $B_{\parallel} = 10$ T, perpendicular to the transport direction and for four different top gate voltages: 0, –0.3 V, –0.5 V, and –0.82 V.

## III. EXPERIMENTAL RESULTS

Figure 1 shows the conductance characteristics of a 1D quantum wire under a symmetric confinement potential and at varying top gate voltages. The inset depicts an optical microscope image of a representative device similar to the one used in this study, which has a pair of split gates and a top gate. At $V_{tg} = 0$ V, although regular quantized conductance plateaus were observed, the effect of impurity scattering was prominently noticed. The conductance trace exhibits a sharp peak, a resonance effect because of a localized impurity, just before the pinch-off, followed by plateaus that deviate slightly from the quantized value of $N\mathrm{G}_0$, where $N$ is an integer and $\mathrm{G}_0 = 2e^2/h$. The plateau associated with the first subband ($\sim 0.9\mathrm{G}_0$) shows irregularities characterized by resonance peaks and dips, potentially connected with the localized impurity in the channel. A similar feature is also present at $\sim 3\mathrm{G}_0$. Moreover, the 0.7 anomaly, which occurs at $\sim 0.6\mathrm{G}_0$, is observed. One prominent observation was that the 0.7-like features, i.e., $\sim 1.6\mathrm{G}_0$, $\sim 3.7\mathrm{G}_0$, and $\sim 4.7\mathrm{G}_0$ are identified in higher-order subbands.

As the electron density decreases with the application of a negative top gate voltage, the resonance in the first plateau at $\sim 0.9\mathrm{G}_0$ weakens and eventually disappears, along with the saturation at $\mathrm{G}_0$ near $V_{tg} = -0.5$ V ($V_{sg} \sim -0.8$ V). At this moderate confinement potential, the 0.7 anomaly has gradually shifted to higher conductance values, strengthened and saturated around $0.8\mathrm{G}_0$. Moreover, plateaus observed at fractional values ($\sim 1.6\mathrm{G}_0$, $\sim 3.7\mathrm{G}_0$, and $\sim 4.7\mathrm{G}_0$) in higher-order subbands shift to higher conductance values under decreasing electron density and merge with integer conductance plateaus (see the dotted lines, Fig. 1). Furthermore, new conductance states emerge in the third subband as $V_{tg}$ varies between −0.3 and −0.5 V.

A reduction in carrier density leads to an increase in the conductance of the peaky structure observed just before pinch-off, reaching a maximum at $0.5\mathrm{G}_0$ ($V_{sg} \sim -0.5$ V). Additionally, as the top gate is made more negative (< –0.6 V), a complex crossing of energy levels is observed similar to what was reported previously [15,21]. It has been suggested that this is the regime where the ground state and the first excited state intersect caused by the presence of symmetric and antisymmetric states. This leads to a new ground state represented by $4e^2/h$ and the emergence of the zigzag arrangement of electrons, essentially resulting in the formation of a 1D Wigner lattice [15,19–21].

It may be noted that plateaus are not finely defined as a result of the longer 1D wire (0.8 μm). The impurity effects on quantization in 1D quantum channels have been extensively documented [23,24]. It was reported that ionized donors may introduce random potential with long-range fluctuations that could smear out conductance plateaus in longer quantum wires (> 0.5 μm). The isolated peak was reported to form just before the pinch-off as a result of resonant tunneling through

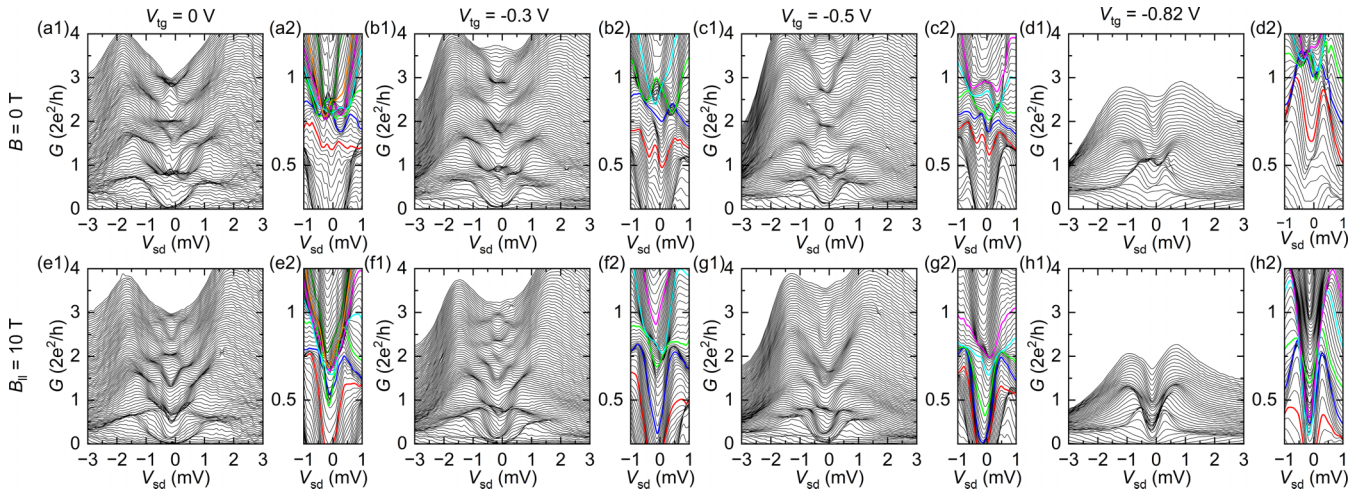


FIG. 2. Conductance characteristics for dc source-drain bias spectroscopy. Differential conductance, $G$, as a function of source-drain bias voltage $V_{sd}$ for different split-gate voltages at zero magnetic field and (a1) $V_{tg} = 0$ V, (b1) $V_{tg} = -0.3$ V, (c1) $V_{tg} = -0.5$ V, and (d1) $V_{tg} = -0.82$ V. Corresponding data at $B_{\|} = 10$ T for different $V_{tg}$ are presented in (e1), (f1), (g1), and (h1), respectively. The data shown here were derived from $G$ *vs* $V_{sg}$ (at different $|V_{sd}| \leqslant 3$ mV) using the method of interpolation. The magnified views of each plot are shown on the right of each plot and labeled as a2, b2.....h2. The magnified plots highlight selected conductance traces with different colors to illustrate the evolution trend under moderate dc source-drain bias. For each top-gate setting, the conductance traces corresponding to identical $V_{sg}$ values are shown using the same colors for $B = 0$ T and $B_{\|} = 10$ T.

the quasibound state of the impurity, that also affected the first plateau as a result of resonant scattering from the impurity [25,26]. We notice a few similarities between our impurity driven features, as in Fig. 1, and the work in Refs. [25,26].

Figure 2 shows the evolution of the conductance characteristics under varying dc source-drain bias for various top gate voltages at $B = 0$ T and $B_{\|} = 10$ T. In this measurement, the bunching of traces, for example, at zero source-drain bias, signifies plateaus observed in conductance measurements. At $V_{tg} = 0$ V and at $B = 0$ T [Fig. 2(a1)], the conductance value at the resonance peak (shown in Fig. 1 as *), that occurs near the pinch-off, essentially increases under rising $|V_{sd}|$, evolving as a semicircle for $|V_{sd}| \lesssim 1$ mV, and eventually merges to the 0.7 anomaly that forms in the nonlinear regime for 1 mV $\lesssim |V_{sd}| \lesssim 2$ mV. It may be noted that because of the presence of disorders, the plateau, especially the $2e^2/h$, is not aligned with the expected value despite removing the series resistance. It has been shown that Luttinger liquid caused by the correlation effects could reduce the conductance quantization to less than $2e^2/h$ [27]. The half-integer plateaus ($1/2 \times N G_0$) emerge in the higher-order subbands ($N \geqslant 2$) for 0.5 mV $\lesssim |V_{sd}| \lesssim$ 1.5 mV, represented as a bunching of traces (the evolution of plateaus with $V_{sd}$ may be visualized in Fig. 4). As the magnitude of the dc bias increases, the chemical potentials of the source and drain shift in opposite directions relative to the equilibrium Fermi level. Half-integer conductance plateaus appear when one of the chemical potentials (either source or drain) exceeds a subband energy level, while the other remains within the subband range [28,29]. Furthermore, the plateau at $\sim 1.6G_0$ (at $V_{sd} = 0$ V) divides into two plateaus at finite source-drain bias, which settle at $\sim 1.8G_0$. This trend is similar to what the integer plateaus generally display when applying a varying source-drain bias, indicating that the $1.6G_0$ exhibits a true 1D subband feature [29].

We noticed that zero-bias anomaly (ZBA) originated from sub-$G_0$ values and appeared in higher subbands. Also, we noted that the bunching of traces close to $G_0$ crosses each other at zero source-drain bias. The magnified view is shown in Fig. 2(a2). We noticed the ZBA peak was absent until close to $0.5G_0$, afterward it evolves, shown in the red trace accompanied by asymmetrically placed neighboring peaks at finite source-drain bias (FB). The complex crossing of satellite and ZBA peaks is indicated by colored traces (blue, green, magenta, orange), showing resonance of competing impurity and 1D states.

As the top gate voltage is made more negative, the plateaus are significantly affected under varying dc source bias voltage. At $V_{tg} = -0.3$ V and at $B = 0$ T, the usual semicircle impurity-driven state is observable at $V_{sd} \simeq 0$ V, followed by a 0.7 feature [Fig. 2(b1)]. The ZBA peak is also present in this case, although it starts appearing at a value lower than $0.5G_0$ and continues to $0.75G_0$. The ZBA peak is accompanied by FB peaks within $|V_{sd}| \lesssim 1$ mV. We noticed the crossing of traces at $G_0$, although less pronounced than compared to $V_{tg} = 0$ V; a gap has occurred in the bunching of traces [seen as forming a ring, enclosed between traces cyan and green, Fig. 2(b2)]. The $1.6G_0$ feature is still present, although relatively weakened compared to $V_{tg} = 0$ V. At $V_{tg} = -0.5$ V, the usual semicircle impurity state is still observable, followed by a 0.7 feature, accompanied by the ZBA and FB peaks [Fig. 2(c1)]. The FB peaks are strongly present, as may be noticed in the plot, and are distinct compared to the impurity-driven semicircle feature that merges with the 0.7 feature under increasing source-drain bias. The crossing of traces that occurred at $V_{tg} = 0$ and –0.3 V, has significantly reduced, forming a distinct gap [between traces blue and magenta, Fig. 2(c2)]. The $1.6G_0$ feature at $V_{sd} = 0$ V has disappeared at this top gate voltage, presumably merged with $2G_0$. At

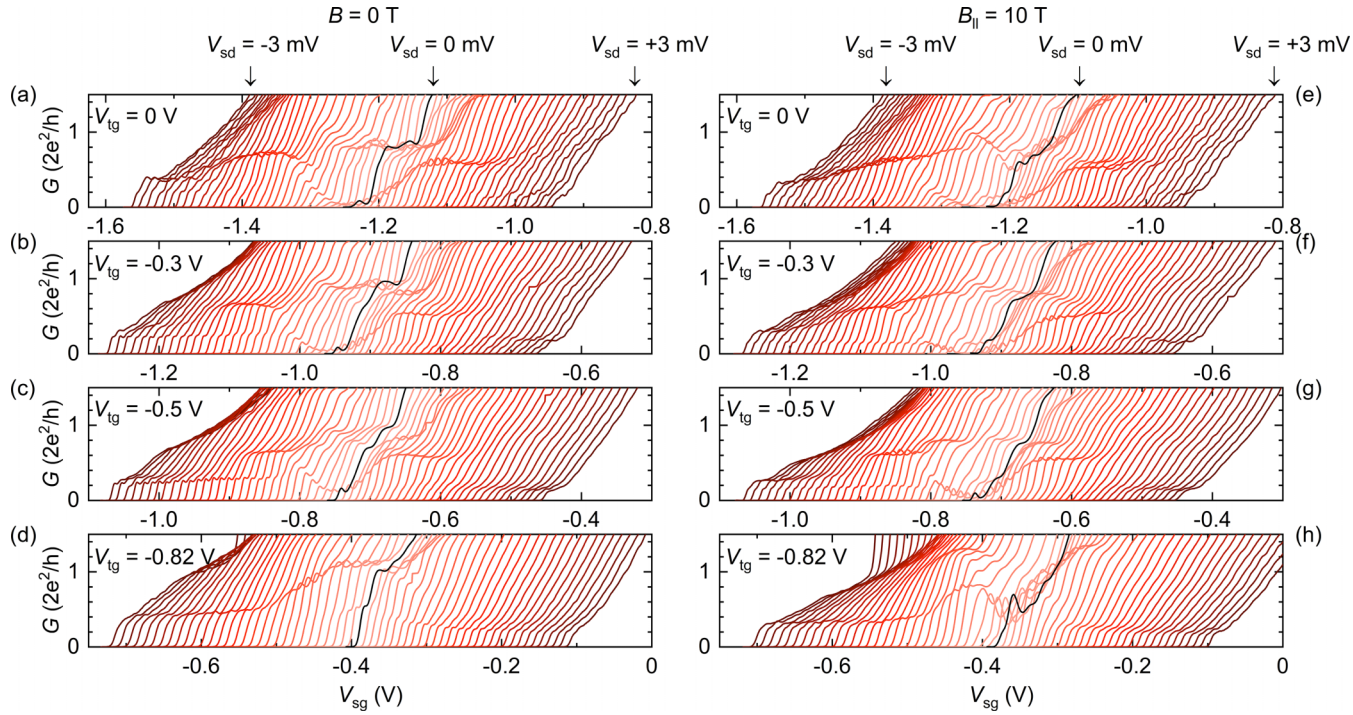


FIG. 3. Conductance characteristics for dc source-drain bias spectroscopy. Differential conductance $G$ as a function of split-gate voltage $V_{sg}$ for source-drain bias voltage $V_{sd}$ at zero magnetic field and (a) $V_{tg} = 0$ V, (b) $V_{tg} = -0.3$ V, (c) $V_{tg} = -0.5$ V, and (d) $V_{tg} = -0.82$ V. Corresponding data at $B_{\parallel} = 10$ T for different $V_{tg}$ are presented in (e), (f), (g), and (h), respectively. For clarity, the conductance traces have been shifted along the $x$ axis by a difference of 0.01 V between each trace along the $x$ axis relative to the trace for $V_{sd} = 0$ V, with shifts to the left for negative $V_{sd}$ and to the right for positive $V_{sd}$. The leftmost trace corresponds to $V_{sd} = -3$ mV and the rightmost to $V_{sd} = 3$ mV, with each successive trace incremented by 0.1 mV from left to right.

$V_{tg} = -0.82$ V, the semicircle effect close to the pinch-off is not visible [Fig. 2(d1,d2)]. The ZBA peak is also missing, though FB peaks are prominently present, which, along with the resonating states, creates a crossing of traces close to $G_0$. Higher subbands were not resolved at this top gate voltage.

At $B_{\parallel} = 10$ T and at $V_{tg} = 0$ V [Fig. 2(e1)], the Zeeman energy lifts the spin degeneracy of the 1D subbands, resulting in the spin-polarized bands quantized at $1/2 \times NG_0$ for $V_{sd} \simeq 0$ V. This spin polarization is prominently visible in the higher subbands, as depicted in the contour plots for clarity [Fig. 4]. The zero field, $1.6G_0$ feature appearing at $V_{sd} \simeq 0$ V, has merged with the $1.5G_0$. The $1.8G_0$ features appearing at FB, emerging from the $1.6G_0$ at zero magnetic field, show interesting evolution at $B_{\parallel} = 10$ T. They have now settled at $1.75G_0$ and the bunching of traces is now robust than at $B = 0$ T, indicating they are spin-polarized states. The quarter plateaus at FB in higher bands ($1.75G_0$, $2.75G_0$) were also resolved [Figs. 2(e1) and 2(f1)]. The resonance peak near the pinch-off has split into two, which indicates that the impurity state is of magnetic origin [30]. This occurs as two semicircles in the plot. The complex bunching of traces has also split distinctively into two, one aligns with $0.5G_0$ and the other $\sim 0.7G_0$ at $V_{sd} = 0$ V [Fig. 2(e1)]. For $V_{tg} = -0.5$ V, where the resonance between the states had already reduced at $B = 0$ T, now at $B_{\parallel} = 10$ T, has completely weakened [Fig. 2(g2)], resulting in a structure close to $0.7G_0$ at $V_{sd} = 0$ V. At $V_{tg} = -0.82$ V, no semicircle trend close to pinch-off was observed, while bunching of traces above and below the $0.5G_0$ was noticed [Fig. 2(h1,h2)]. The crossing of traces or resonance at $G_0$ has smeared out. For all top gate voltages, the ZBA peak and the resonance peaks that were prominent at zero magnetic field, disappeared. It may be noted that despite a strong $B_{\parallel} = 10$ T, the bunching of traces or plateau close to the spin-polarized $0.5G_0$ state was not observed for negative top gate voltages. It may be worth mentioning that the semicircle-shaped impurity-driven effects observed close to pinching off at $V_{sd} \simeq 0$ V, as in Figs. 2(a1)–2(d1), resemble the typical in-plane magnetic field introduced effects [31] [see Figs. 2(e1)–2(h1)], perhaps indicating the impurities in the channel are magnetic in nature.

To investigate the effect of large source-drain bias on conductance characteristics, we will consider the results of conductance as a function of split-gate voltage for varying source-drain bias, and mainly focus on the effect for 1 mV $\lesssim |V_{sd}| \leqslant 3$ mV, as shown in Fig. 3 for both $B = 0$ T and $B_{\parallel} = 10$ T. At $V_{tg} = 0$ V, Fig. 3(a), as the source-drain bias increases negatively toward –3 mV, two conductance structures below $0.5G_0$ were resolved, roughly indexed at $0.4G_0$ ($4/5e^2/h$) and $0.2G_0$ ($2/5e^2/h$). On the application of gradually increasing positive $V_{sd}$ to 3 mV, only one structure approximately at $0.2G_0$ ($2/5e^2/h$) is resolved. With $B_{\parallel} = 10$ T, Fig. 3(e), the dual conductance structures toward $V_{sd} = -3$ mV, and a single structure towards $V_{sd} = 3$ mV persist, although their magnitude has slightly reduced. At $V_{tg} = -0.3$ V and $B = 0$ T [Fig. 3(b)], a plateau $\sim 0.25G_0$ appears at $V_{sd} \simeq -1$ mV, which remains persistent on increasing $V_{sd}$ negatively to –3 mV. Moreover, a second plateau around $0.4G_0$ arises with a subtle interbound state (at $\sim 0.3G_0$) for –3 mV $\lesssim V_{sd} \lesssim$ –2 mV. At positive dc bias voltage, plateaus at $\sim 0.1G_0$ and

$\sim$0.2$G_0$ appear for $V_{sd} \gtrsim 1$ mV and $V_{sd} \gtrsim 2$ mV, respectively. At $B_\parallel = 10$ T, $V_{tg} = -0.3$ V [Fig. 3(f)], for the negative dc bias voltage, a plateau at $\sim$0.16$G_0$ arises for $V_{sd} \lesssim -1$ mV. A faint signature of the 0.25$G_0$ ($1/2e^2/h$) state is noticeable for $V_{sd} < -2.5$ mV. Further, the 0.5$G_0$ state is present at $V_{sd} \simeq -2$ mV, which monotonically reduces to lower conductance values under more negative biasing and finally saturates at $\sim$0.25–0.3$G_0$ for $V_{sd} < -2.5$ mV. On the other hand, with positive dc bias voltages, plateaus occur at $\sim$0.08$G_0$ ($1/6e^2/h$) and 0.2$G_0$($2/5e^2/h$) for 1 mV $\lesssim V_{sd} \leqslant 3$ mV and 2 mV $\lesssim V_{sd} \leqslant 3$ mV, respectively.

A further decrease in the top gate voltage, $V_{tg} = -0.5$ V, Fig. 3(c), at $B = 0$ T, yields a resonance peak at $\sim$0.3$G_0$ for –2 mV $\lesssim V_{sd} \lesssim -1$ mV. For –3 mV $\leqslant V_{sd} \lesssim$ –2 mV, the resonance peak reduces to lower conductance values, and the plateau at $\sim$0.3$G_0$ becomes distinguishable along with intervening states for –3 mV $\leqslant V_{sd} \lesssim$ –2.5 mV, resonating between 0.3 and 0.25$G_0$. In contrast, with a positive bias voltage for $V_{sd} > 1$ mV, a prominent plateau occurs at $\sim$0.16$G_0$. At $B_\parallel = 10$ T, Fig. 3(g), and under negative biasing, a $\sim$0.2$G_0$ state appears for –1.5 mV $\lesssim V_{sd} \lesssim -1$ mV, which transforms into states with conductance of $\sim$0.16$G_0$ ($1/3e^2/h$) and $\sim$0.3$G_0$ ($3/5e^2/h$) for –3 mV $\leqslant V_{sd} \lesssim$ –1.5 mV. However, positive biasing displays plateaus at $\sim$0.16$G_0$ ($1/3e^2/h$) for $V_{sd} \gtrsim 1.5$ mV. At a very large top gate voltage, $V_{tg} = -0.82$ V, Figs. 3(d) and 3(h), a state $\sim$0.4–0.5$G_0$ is stable for –3 mV $\leqslant V_{sd} < -1.5$ mV at $B = 0$ T, with a subtle 0.33$G_0$ state also occurring at –3 mV $\leqslant V_{sd} < -2.5$ mV. Under positive bias, stable 0.22$G_0$ and 0.33$G_0$ states occur for $V_{sd} > 1.7$ mV. With $B_\parallel = 10$ T, 0.25$G_0$ ($1/2e^2/h$) and 0.33$G_0$ ($\sim 3/5e^2/h$) states are observed for –3 mV $\leqslant V_{sd} \leqslant$ –2 mV and 0.2–0.25$G_0$ ($\sim 1/2e^2/h$) state for $V_{sd} > 2$ mV.

For discussion purposes, we restrict ourselves to two conductance structures appearing at large dc bias ($|V_{sd}| \geqslant 2$ mV) around 0.2$G_0$ and 0.4$G_0$ for $V_{tg} = -0.5$ V [Fig. 3(c)]. These features are more pronounced for negative $V_{sd}$ compared to positive $V_{sd}$. Previously, such dual conductance structures appearing close to 0.25$G_0$ and 0.5$G_0$ were reported [1,15,19–21]. The plateau at 0.25$G_0$ is known to arise from the lifting of both momentum and spin degeneracy under large dc bias [32]. The additional plateau at 0.5$G_0$ has been considered a result of the formation of two separate electron rows under enhanced Coulomb interactions, leading to a Wigner lattice structure in one-dimensional channels [20,21]. The observed shift in the dual conductance plateaus in our results may be caused by correlation effects and perhaps disorders, that do not destroy these structures but modify them by shifting to lower conductance values resembling fractional states (in units of $e^2/h$) 2/5 and 4/5. Determining whether they are the actual fractional states necessitates a thorough investigation, which is outside the scope of this article. It is important to note that the signature of Wigner crystallization is not present in the linear transport regime. At a high bias voltage, the carrier distribution shifts out of equilibrium and populates higher 1D subbands. This redistribution enhances both the inter- and intraband interactions and increases the correlation effects with increasing bias voltage. In addition, screening decreases owing to the depletion of low-energy electrons, leading to stronger Coulomb interactions. These conditions may promote the occurrence of correlated phases, such as Wigner crystallization, which could be suppressed or less pronounced in the linear transport regime.

It may be noted from Fig. 3, left panel plots for $B = 0$ T, that the two conductance structures appearing at the large negative source-drain bias, gradually move closer to each other, i.e., the conductance gap between them reduces on reducing carrier density as the top gate is made more negative. This may be noticed from Fig. 3(c), $V_{tg} = -0.5$ V, where the two conductance structures have come close enough to form hybrid states, resulting in resonance between the intervening states. When the density is further reduced, at $V_{tg} = -0.82$ V, the two states may have merged to form a degenerate single state. This discussion may also be applied to $B_\parallel = 10$ T plots. However, the magnetic field induces noticeable shifts in the conductance values of these dual states [33].

We noted the dual fractional-like states emerge at higher source-drain bias for decreasing carrier density in the 1D channel. On the other hand, the higher-order derivatives of the 0.7 structure, at zero source-drain bias, also become pronounced when the carrier density is reduced. This indicates enhanced correlation effects including exchange interactions arising by the reduced number of electrons in the channel. However, the asymmetry in the intensity of these features and quantitative differences in their appearance for negative and positive biases may arise because of multiple reasons such as asymmetry in the channel, inhomogeneity in the background potential, and nonlinearity assisted by disorders in longer and wider quantum wires [34–36]. It was suggested that the conductance asymmetry could be related to the asymmetric effect of an applied electric field and its distribution within the quantum system, and their coupling to the Fermi liquid outside the 1D wire [37].

Figure 4 shows the contour plots of the transconductance $dG/dV_{sg}$ as a function of $V_{sd}$ and $V_{sg}$ for $V_{tg} = 0$ V and –0.3 V both for $B = 0$ T and $B_\parallel = 10$ T. In the linear regime ($V_{sd} \simeq 0$ V), up to four 1D subbands are identified. Under increasing dc bias, the chemical potentials of the source and drain shift in opposite directions relative to the equilibrium Fermi level. When the applied bias exceeds the subband spacing, this results in the appearance of half-integer conductance plateaus. The $V_{sd}$ values at the crossing points of the diamonds reflect the energy spacings between the subsequent subbands. The 0.7 structure and its derivatives in higher subbands are visible for $V_{tg} = 0$ V. It becomes more prominent as the top gate voltage decreases [e.g., Fig. 1], suggesting the enhanced interactions between electrons. The spin-polarized subbands are resolved at $B_\parallel = 10$ T, mostly in higher-order subbands.

In order to further understand the conductance characteristics quantitatively, we estimated the subband spacings and electron density of the 1D wire. The energy spacings between the consecutive subbands, $E_{N+1} - E_N = e(|V_{sd}^+| + |V_{sd}^-|)/2$, were calculated from the $V_{sd}$ values corresponding to crossing points of the diamonds observed in the contour plots of the dc source-drain bias measurements [see Fig. 4], where $|V_{sd}^+|$ and $|V_{sd}^-|$ are the values at the positive and negative $V_{sd}$, respectively. Here, $N$ denotes the subband index ($\geqslant 1$). Furthermore, knowing the pinch-off voltage for the symmetric split-gates configuration, the variation of electron density in the 2DEG $n_{2D}$ for different applied top gate voltage was estimated

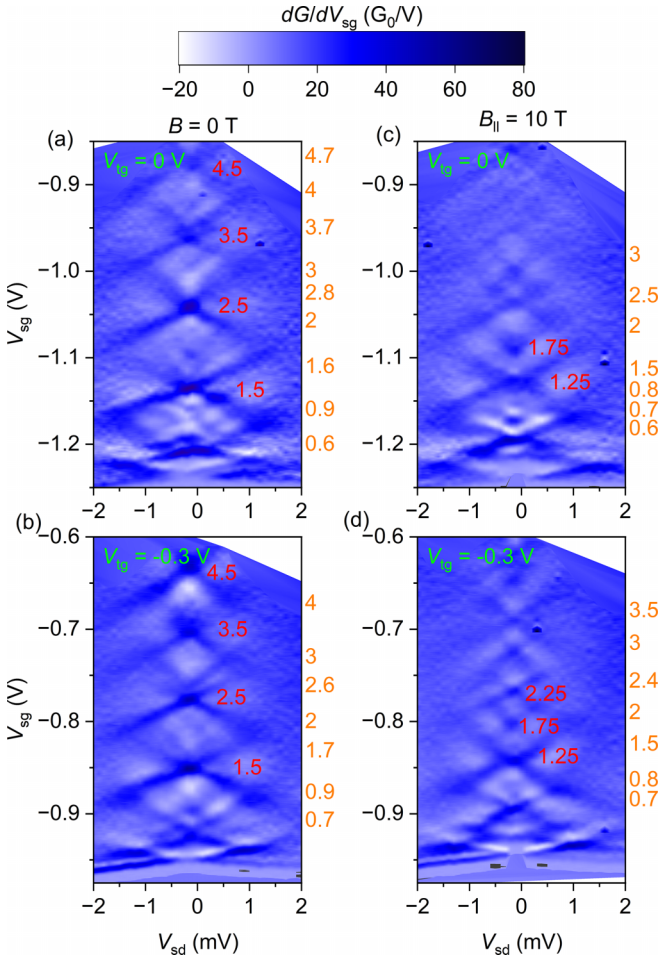


FIG. 4. Contour plots of the transconductance, $dG/dV_{sg}$, as a function of $V_{sd}$ and $V_{sg}$ for (a) $V_{tg} = 0$ V and (b) $V_{tg} = -0.3$ V at zero magnetic field. Corresponding plots for $B_{\parallel} = 10$ T are shown in (c) and (d), respectively. All plateaus at $V_{sd} \simeq 0$ V across the plot have been indexed in units of $2e^2/h$, labeled on the right $y$ axis for each plot. A few half-integer states are indexed within the plot for clarity.

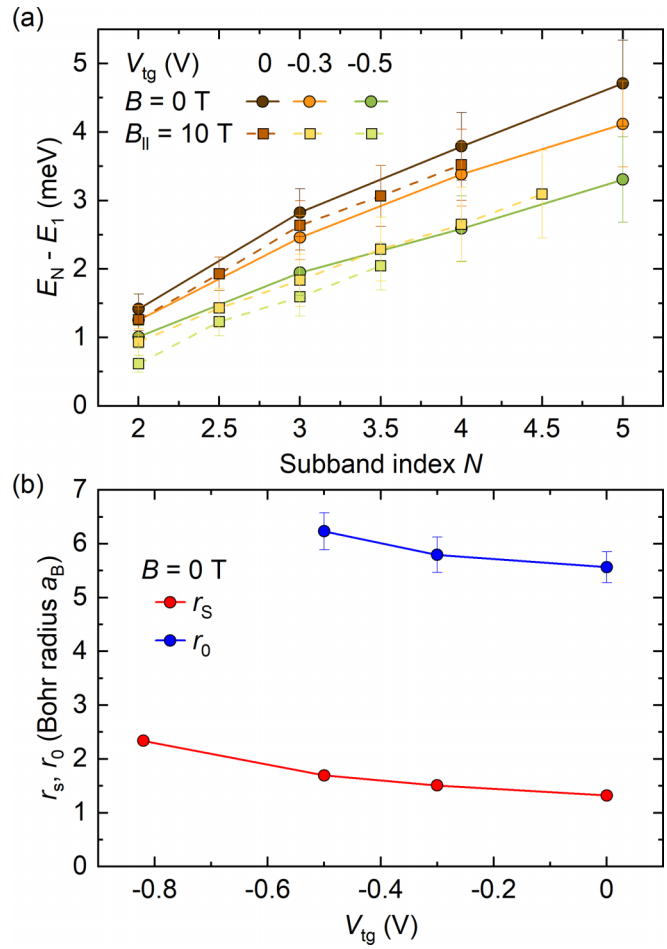


FIG. 5. Evolution of 1D parameters calculated for different top gate voltages. (a) Energy spacing between the subband $N$ and the ground state ($N = 1$) at $B = 0$ and $B_{\parallel} = 10$ T obtained from the dc source-drain bias data. (b) Wigner-Seitz radius $r_s$, and the confinement parameter $r_0$ estimated at $B = 0$ T.

using the relation $n_{2D} = (\epsilon/2\pi eD)V_P$, where $\epsilon$ (= 12.9) is the dielectric constant of GaAs, e is the electron charge, $D$ (= 0.5 μm) is the distance between the split gates, and $V_P$ is the pinch-off voltage [38]. For simplicity, assuming a square well confinement in the transverse direction, the width of the 1D channel $W$ is then approximated as $\lambda_{2D}/2$ when only the first subband is occupied. Here, $\lambda_{2D} = (2\pi/n_{2D})^{1/2}$ is the Fermi wavelength of the 2DEG. The electron density of the 1D wire, $n_{1D} = n_{2D}W$, is therefore estimated.

Figure 5 shows the obtained 1D parameters for different top gate voltages at $B = 0$ T and $B_{\parallel} = 10$ T. The energy spacing between the subband $N$ ($\geqslant 1$) and ground state ($N = 1$), $E_N - E_1$, deviates from the straight line behavior [Fig. 5(a)], a feature of the parabolic confinement (equally spaced subbands). Higher-order subbands are closely spaced compared to lower-order subbands, revealing that the confinement potential is not a perfect parabola. Applying a more negative $V_{tg}$ and a magnetic field further reduces the subband spacings. Nonetheless, the confinement potential parameter, $r_0 = (2e^2/\epsilon m^* \omega^2)^{1/3}$, is roughly estimated, where $m^*$ is the effective mass of electrons in GaAs and $\omega$ (= $(E_2$-$E_1)/\hbar$) is the frequency of the confinement potential (parabolic) [8,9]. Figure 5(b) shows the variation of Wigner-Seitz radius $r_s$ (=$1/n_{1D}$) and parameter $r_0$ in units of Bohr radius $a_B$, for $B = 0$ T. The $r_s \geqslant 1$ suggests a possible formation of a Wigner lattice in the 1D channel. As $r_0 \approx 4r_s$, the formation of two parallel electron rows ($r_0 > r_s$) from the zigzag structure ($r_0 \approx r_s$) is plausible. It is worth noting that Wigner crystallization in higher-dimensional systems requires much larger $r_s$ values ($\sim 37a_B$ in two dimensions [39] and $\sim 100a_B$ in three dimensions [40]), as the increased phase space allows electrons to minimize mutual repulsion more effectively, thereby reducing correlation effects. In contrast, the more confined geometry in 1D enhances Coulomb interactions and can allow crystallization at much lower $r_s$ [8–13]. Using quantum Monte Carlo simulation, Mehta *et al.* [9] demonstrated a transition from a linear to zigzag configuration in 1D as Wigner radius varies from $\sim 1a_B$ to $\sim 4a_B$ under different electron densities. Based on the estimated $n_{1D}$ in our result, the interaction energy of the electrons is stronger ($\propto n_{1D}$) compared to the kinetic energy (Fermi energy $\propto n_{1D}^2$) in the ground state. The observed features, such as the dual conductance structures at large dc bias, result from

electron-electron interactions, which strengthen at a more negative top gate voltage.

## IV. DISCUSSION

The observation of the 0.7 anomaly in the conductance of 1D quantum wires has been proposed to arise from various mechanisms, low-density intrinsic spin polarization, Kondo physics caused by localized impurities, or a combination of both, the Wigner lattice, etc. [41,42]. The 0.7 anomaly generally develops into a 0.5 feature on the application of an in-plane magnetic field, suggesting a ferromagnetic ordering caused by aligned spins [6]. It was reported that in the 2DEG, at low densities, the exchange interaction drives electrons spin to align in one direction [43]. Berggren, Yakimenko, and Wang [44,45] calculated that in a 1D channel, as a result of exchange and correlation effects, a spin gap is created, leaving the system to populate parallel spin-down states to lower its energy. This is a case of intrinsic spin polarization without any magnetic field. Similarly, Reilly [46] suggested through a phenomenological model that a spin gap is formed in the 1D system as a function of 1D carrier density. It was indicated that the spin gap increases with $E_F$, implying the appearance of higher order 0.7 structures, as seen in the present work.

It was also reported that anomalous features developed at the crossing of the 1D subbands threshold because of Zeeman energy in the presence of a high in-plane magnetic field. These anomalous conductance features were developing similarly to the way the 0.7 anomaly was gradually developing into the $0.5G_0$ feature on increasing the in-plane magnetic field [47,48]. These so-called "0.7 analog" were attributed to exchange and Coulomb interactions arising from the low-density regime [41,49]. This is an important indication that exchange and correlation effects may still show dominance in 1D systems despite the presence of the substantial Zeeman Effect.

In the present work, we have identified the presence of the 0.7-like anomaly at higher subbands, namely $1.6G_0$, $3.7G_0$, and $4.7G_0$, and they were found to merge with the integer plateaus on lowering the carrier density in the 1D channel. They may have appeared because of the possibility of exchange and correlation effects at higher subbands [44,45], based on the calculation utilizing the Kohn-Sham (KS) local spin-density approach (LSDA). It is argued that at low density in the 1D channel, near the pinch-off, both spin-up and spin-down states are present, as the split gate voltage is relaxed, so the ground state starts getting populated, because of the exchange correlation, the spin-down subband gets populated first resulting in the 0.7 feature. The remaining electrons populate the next subband as the Fermi level is moved up using the split gate voltage. As the Fermi level enters the second subband, when it crosses a subband threshold energy, the spin splitting could be pronounced owing to the exchange potential, resulting in the observation of additional spin-split states at higher subbands, namely $1.6G_0$, $3.7G_0$, and $4.7G_0$.

The longer quantum wires (2 μm) were reported to exhibit enhanced spin splitting with the 0.7 structure being close to the $0.5G_0$, although resonating, and signatures of higher order 0.7 structures or derivatives in the second subband at $1.7G_0$; the effects were attributed to many-body physics within the 1D channel [50]. In another report, similar 0.7 derivatives in the first and second subbands were reported in 0.31 μm long quantum wires, and the effect was attributed to the disorders from the donor layer at a distance of 15 nm from the 2DEG [51]. In the present work, despite the donor layer being 40 nm apart from the 2DEG, the disorder effects from the donor layer and inhomogeneity in the background potentials may not be ignored, as they depend on various parameters, such as the cooldown process, the rate at which gate voltages are swept, the associated electric field, etc.

In our results with in-plane magnetic field at $B_{\parallel} = 10\,\mathrm{T}$, we did observe the spin-polarized conductance plateaus for different negative top gate voltages, in higher subbands, however, in the ground state, the spin-polarized state was not found at $0.5G_0$. It is known that the $g$ factor within the 1D channel and across its different subbands vary significantly [6]. The $g$ factor also appears to vary with the carrier density. Calculations of the exchange potential in a square confining potential have shown that the effective $g$ factor decreases when the 1D confining potential weakens and the 2D limit is approached [52,53]. At a lower electron density (negative top gate voltage), and in the lowest subband, the exchange energy can become significant when an aligned spin subband has formed despite the presence of Zeeman energy. Moreover, the correlation energy and impurity effects might also inhibit the complete transmission through the lower spin subband. Thus, weakly defined spin-split features were noticed in the ground state compounded by resonance features from the bound states in the channel.

We noticed ZBA peaks across several subbands in our samples. Along with ZBA, satellite peaks around $V_{sd} = \pm$ 1 mV were also seen, similar to the one reported by Sfigakis *et al.* [7], attributed to resonance states from the impurities in the channel [7,54]. We argue that the impurity states present in our system influence the transmission through the channel. On applying a finite source-drain bias, the transmission through the channel is modified when the impurity states and 1D subbands align, resulting in resonant states. It may be noted that clean 1D systems were reported to show ZBAs with and without satellite peaks, implying ZBA is intrinsic to 1D wires. The reduced ZBA peak, as in our case, could be attributed to low electron density, electric field distribution, impurity effects, and so on [51,54,55]. There are conflicting reports on whether the ZBA peak is caused by Kondo physics [31] or non-Kondo [56]. Sfigakis *et al.* [7] performed measurements on a 1D quantum wire and showed that both the Kondo and non-Kondo 0.7-related effects give rise to the ZBA peak. On the application of an in-plane magnetic field, the ZBA peaks disappeared in our case, contrary to reports where the ZBA divides into two [31]. Wen *et al.* reported for a disordered 1D quantum wire, the ZBA peak was suppressed similar to our case [51]. However, when they moved away from the disordered state, the split in the ZBA was revived, unlike in our case as the ZBA had suppressed for the entire confinement regime. We suspect the suppression of ZBA in our case could be derived from low-density and strong correlation effects, including exchange, and of course, the impurity effects cannot be ruled out. It was also suggested that the suppression of ZBA may arise because of the underlying $g$-factor anisotropy of the 1D quantum wire [57].

## V. CONCLUSIONS

In conclusion, we presented the results of transport measurements in a longer quantum wire, where the disorder-induced correlation effects were investigated. We observed the 0.7 conductance anomaly in the ground state and its siblings at higher subbands, most likely because of an exchange correlation in the system. A detailed source-drain bias spectroscopy at zero and 10 T in-plane magnetic field identified two conductance states at large dc bias. These states become more pronounced with the appearance of higher derivatives of the 0.7 structure at zero field under reducing electron density, indicating the influence of strong correlation effects on their formation. The observed quantitative changes in conductance plateaus and essentially qualitative similar features in both positive and negative dc biases suggest that impurities play a significant role in mediating interactions between electrons. Also, strong signatures of dual conductance states, resembling the fractional states at $0.2G_0$ and $0.4G_0$, at large dc bias suggest that the 1D channel hosts a Wigner lattice in the low-density regime.

## ACKNOWLEDGMENTS

The work is funded by the United Kingdom Research and Innovation (UKRI), Future Leaders Fellowship (References No. MR/S015728/1; No. MR/X006077/1), the Engineering and Physical Sciences Research Council (EPSRC), the Royal Society and the Science and Technology Facilities Council, STFC (Reference No. ST/Y005147/1).

## DATA AVAILABILITY

The data that support the findings of this article are openly available [58].

[1] S. Kumar and M. Pepper, Interactions and non-magnetic fractional quantization in one-dimension, Appl. Phys. Lett. **119**, 110502 (2021).

[2] K.-F. Berggren and M. Pepper, Electrons in one dimension, Philos. Trans. R. Soc. A **368**, 1141 (2010).

[3] T. J. Thornton, M. Pepper, H. Ahmed, D. Andrews, and G. J. Davies, One-dimensional conduction in the 2D electron gas of a GaAs-AlGaAs heterojunction, Phys. Rev. Lett. **56**, 1198 (1986).

[4] D. A. Wharam, T. J. Thornton, R. Newbury, M. Pepper, H. Ahmed, J. E. F. Frost, D. G. Hasko, D. C. Peacock, D. A. Ritchie, and G. A. C. Jones, One-dimensional transport and the quantisation of the ballistic resistance, J. Phys. C: Solid State Phys. **21**, L209 (1988).

[5] B. J. van Wees, H. Van Houten, C. W. J. Beenakker, J. G. Williamson, L. P. Kouwenhoven, D. van der Marel, and C. T. Foxon, Quantized conductance of point contacts in a two-dimensional electron gas, Phys. Rev. Lett. **60**, 848 (1988).

[6] K. J. Thomas, J. T. Nicholls, M. Y. Simmons, M. Pepper, D. R. Mace, and D. A. Ritchie, Possible spin polarization in a one-dimensional electron gas, Phys. Rev. Lett. **77**, 135 (1996).

[7] F. Sfigakis, C. J. B. Ford, M. Pepper, M. Kataoka, D. A. Ritchie, and M. Y. Simmons, Kondo effect from a tunable bound state within a quantum wire, Phys. Rev. Lett. **100**, 026807 (2008).

[8] J. S. Meyer and K. A. Matveev, Wigner crystal physics in quantum wires, J. Phys.: Condens. Matter **21**, 023203 (2009).

[9] A. C. Mehta, C. J. Umrigar, J. S. Meyer, and H. U. Baranger, Zigzag phase transition in quantum wires, Phys. Rev. Lett. **110**, 246802 (2013).

[10] B. Brun, F. Martins, S. Faniel, B. Hackens, G. Bachelier, A. Cavanna, C. Ulysse, A. Ouerghi, U. Gennser, D. Mailly *et al.*, Wigner and Kondo physics in quantum point contacts revealed by scanning gate microscopy, Nat. Commun. **5**, 4290 (2014).

[11] L. Shulenburger, M. Casula, G. Senatore, and R. M. Martin, Correlation effects in quasi-one-dimensional quantum wires, Phys. Rev. B **78**, 165303 (2008).

[12] M. Ostilli and C. Presilla, Wigner crystallization of electrons in a one-dimensional lattice: A condensation in the space of states, Phys. Rev. Lett. **127**, 040601 (2021).

[13] H. Montagu, I. Farrer, D. Ritchie, and S. Kumar, Spin polarised quantum conductance in 1D channels, Appl. Phys. Express **18**, 015002 (2025).

[14] S. Kumar, M. Pepper, D. Ritchie, I. Farrer, and H. Montagu, Formation of a non-magnetic, odd-denominator fractional quantized conductance in a quasi-one-dimensional electron system, Appl. Phys. Lett. **115**, 123104 (2019).

[15] S. Kumar, M. Pepper, S. N. Holmes, H. Montagu, Y. Gul, D. A. Ritchie, and I. Farrer, Zero-magnetic field fractional quantum states, Phys. Rev. Lett. **122**, 086803 (2019).

[16] G. Piacente, G. Q. Hai, and F. M. Peeters, Continuous structural transitions in quasi-one-dimensional classical Wigner crystals, Phys. Rev. B **81**, 024108 (2010).

[17] G. Piacente and F. M. Peeters, Pinning and depinning of a classic quasi-one-dimensional Wigner crystal in the presence of a constriction, Phys. Rev. B **72**, 205208 (2005).

[18] I. M. Ruzin, S. Marianer, and B. I. Shklovskii, Pinning of a two-dimensional Wigner crystal by charged impurities, Phys. Rev. B **46**, 3999 (1992).

[19] W. K. Hew, K. J. Thomas, M. Pepper, I. Farrer, D. Anderson, G. A. C. Jones, and D. A. Ritchie, Incipient formation of an electron lattice in a weakly confined quantum wire, Phys. Rev. Lett. **102**, 056804 (2009).

[20] L. W. Smith, W. K. Hew, K. J. Thomas, M. Pepper, I. Farrer, D. Anderson, G. A. C. Jones, and D. A. Ritchie, Row coupling in an interacting quasi-one-dimensional quantum wire investigated using transport measurements, Phys. Rev. B **80**, 041306(R) (2009).

[21] S. Kumar, K. J. Thomas, L. W. Smith, M. Pepper, G. L. Creeth, I. Farrer, D. Ritchie, G. Jones, and J. Griffiths, Many-body effects in a quasi-one-dimensional electron gas, Phys. Rev. B **90**, 201304(R) (2014).

[22] C. Yan, S. Kumar, K. Thomas, P. See, I. Farrer, D. Ritchie, J. Griffiths, G. Jones, and M. Pepper, Engineering the spin polarization of one-dimensional electrons, J. Phys.: Condens. Matter **30**, 08LT01 (2018).

[23] J. A. Nixon, J. H. Davies, and H. U. Baranger, Breakdown of quantized conductance in point contacts calculated using realistic potentials, Phys. Rev. B **43**, 12638 (1991).

[24] E. Tekman and S. Ciraci, Theoretical study of transport through a quantum point contact, Phys. Rev. B **43**, 7145 (1991).

[25] P. L. McEuen, B. W. Alphenaar, R. G. Wheeler, and R. N. Sacks, Resonant transport effects due to an impurity in a narrow constriction, Surf. Sci. **229**, 312 (1990).

[26] A. Micolich, What lurks below the last plateau: experimental studies of the $0.7 \times 2e^2/h$ conductance anomaly in one-dimensional systems, J. Phys.: Condens. Matter **23**, 443201 (2011).

[27] S. Tarucha, T. Honda, and T. Saku, Reduction of quantized conductance at low temperatures observed in 2 to 10 μm-long quantum wires, Solid State Commun. **94**, 413 (1995).

[28] N. K. Patel, J. T. Nicholls, L. Martn-Moreno, M. Pepper, J. E. F. Frost, D. A. Ritchie, and G. A. C. Jones, Evolution of half plateaus as a function of electric field in a ballistic quasi-one-dimensional constriction, Phys. Rev. B **44**, 13549 (1991).

[29] L. I. Glazman and A. V. Khaetskii, Nonlinear quantum conductance of a lateral microconstraint in a heterostructure, Europhys. Lett. **9**, 263 (1989).

[30] T. Rejec and Y. Meir, Magnetic impurity formation in quantum point contacts, Nature (London) **442**, 900 (2006).

[31] S. M. Cronenwett, H. J. Lynch, D. Goldhaber-Gordon, L. P. Kouwenhoven, C. M. Marcus, K. Hirose, N. S. Wingreen, and V. Umansky, Low-temperature fate of the 0.7 structure in a point contact: A Kondo-like correlated state in an open system, Phys. Rev. Lett. **88**, 226805 (2002).

[32] T.-M. Chen, A. C. Graham, M. Pepper, I. Farrer, and D. A. Ritchie, Bias-controlled spin polarization in quantum wires, Appl. Phys. Lett. **93**, 032102 (2008).

[33] K.-F. Berggren, T. J. Thornton, D. J. Newson, and M. Pepper, Magnetic depopulation of 1D subbands in a narrow 2D electron gas in a GaAs:AlGaAs heterojunction, Phys. Rev. Lett. **57**, 1769 (1986).

[34] T. Heinzel, D. A. Wharam, F. M. de Aguiar, J. P. Kotthaus, G. Bohm, W. Klein, G. Trankle, and G. Weimann, Current-voltage characteristics of quantum point contacts in the high-bias regime, Semicond. Sci. Technol. **9**, 1220 (1994).

[35] A. Kristensen, H. Bruus, A. E. Hansen, J. B. Jensen, P. E. Lindelof, C. J. Marckmann, J. Nygård, C. B. Sørensen, F. Beuscher, A. Forchel, and M. Michel, Bias and temperature dependence of the 0.7 conductance anomaly in quantum point contacts, Phys. Rev. B **62**, 10950 (2000).

[36] H. Kothari, A. Ramamoorthy, R. Akis, S. M. Goodnick, D. K. Ferry, J. L. Reno, and J. P. Bird, Linear and nonlinear conductance of ballistic quantum wires with hybrid confinement, J. Appl. Phys. **103**, 013701 (2008).

[37] H. Linke, W. D. Sheng, A. Svensson, A. Löfgren, L. Christensson, H. Q. Xu, P. Omling, and P. E. Lindelof, Asymmetric nonlinear conductance of quantum dots with broken inversion symmetry, Phys. Rev. B **61**, 15914 (2000).

[38] L. I. Glazman and I. A. Larkin, Lateral position control of an electron channel in a split-gate device, Semicond. Sci. Technol. **6**, 32 (1991).

[39] B. Tanatar and D. M. Ceperley, Ground state of the two-dimensional electron gas, Phys. Rev. B **39**, 5005 (1989).

[40] D. M. Ceperley and B. J. Alder, Ground state of the electron gas by a stochastic method, Phys. Rev. Lett. **45**, 566 (1980).

[41] K.-F. Berggren, P. Jaksch, and I. Yakimenko, Effects of electron interactions at crossings of zeeman-split subbands in quantum wires, Phys. Rev. B **71**, 115303 (2005).

[42] A. D. Klironomos, J. S. Meyer, T. Hikihara, and K. A. Matveev, Spin coupling in zigzag Wigner crystals, Phys. Rev. B **76**, 075302 (2007).

[43] A. Ghosh, C. J. B. Ford, M. Pepper, H. E. Beere, and D. A. Ritchie, Possible evidence of a spontaneous spin polarization in mesoscopic two-dimensional electron systems, Phys. Rev. Lett. **92**, 116601 (2004).

[44] C.-K. Wang and K.-F. Berggren, Spin splitting of subbands in quasi-one-dimensional electron quantum channels, Phys. Rev. B **54**, R14257 (1996).

[45] K.-F. Berggren and I. I. Yakimenko, Nature of electron states and symmetry breaking in quantum point contacts according to the local spin density approximation, J. Phys.: Condens. Matter **20**, 164203 (2008).

[46] D. J. Reilly, Phenomenological model for the 0.7 conductance feature in quantum wires, Phys. Rev. B **72**, 033309 (2005).

[47] A. C. Graham, K. J. Thomas, M. Pepper, M. Y. Simmons, D. A. Ritchie, K.-F. Berggren, P. Jaksch, A. Debnarova, and I. I. Yakimenko, 0.7 analogue structures and exchange interactions in quantum wires, Solid State Commun. **131**, 591 (2004).

[48] A. C. Graham, K. J. Thomas, M. Pepper, N. R. Cooper, M. Y. Simmons, and D. A. Ritchie, Interaction effects at crossings of spin-polarized one-dimensional subbands, Phys. Rev. Lett. **91**, 136404 (2003).

[49] L. Weidinger, C. Schmauder, D. H. Schimmel, and J. von Delft, Functional renormalization group treatment of the 0.7 analog in quantum point contacts, Phys. Rev. B **98**, 115112 (2018).

[50] D. J. Reilly, G. R. Facer, A. S. Dzurak, B. E. Kane, R. G. Clark, P. J. Stiles, A. R. Hamilton, J. L. O'Brien, N. E. Lumpkin, L. N. Pfeiffer, and K. W. West, Many-body spin-related phenomena in ultra low-disorder quantum wires, Phys. Rev. B **63**, 121311(R) (2001).

[51] C.-S. Wen, J. H. Hsiao, and J.-C. Chen, Non-Kondo zero-bias anomaly in disordered quantum wires, J. Appl. Phys. **115**, 063704 (2014).

[52] A. Majumdar, Spin polarization and enhancement of the effective $g$-factor in one-dimensional electron systems with an in-plane magnetic field, J. Appl. Phys. **83**, 297 (1998).

[53] E. J. Koop, A. I. Lerescu, J. Liu, B. J. van Wees, D. Reuter, A. D. Wieck, and C. H. van der Wal, The influence of device geometry on many-body effects in quantum point contacts: Signatures of the 0.7 anomaly, exchange and Kondo, J. Supercond. Novel Magn. **20**, 433 (2007).

[54] K. M. Liu, C. H. Juang, V. Umansky, and S. Y. Hsu, Effect of impurity scattering on the linear and nonlinear conductances of quasi-one-dimensional disordered quantum wires by asymmetrically lateral confinement, J. Phys.: Condens. Matter **22**, 395303 (2010).

[55] S. Sarkozy, F. Sfigakis, K. Das Gupta, I. Farrer, D. A. Ritchie, G. A. C. Jones, and M. Pepper, Zero-bias anomaly in quantum wires, Phys. Rev. B **79**, 161307(R) (2009).

[56] T.-M. Chen, A. C. Graham, M. Pepper, I. Farrer, and D. A. Ritchie, Non-Kondo zero-bias anomaly in quantum wires, Phys. Rev. B **79**, 153303 (2009).

[57] O. Klochan, A. P. Micolich, A. R. Hamilton, K. Trunov, D. Reuter, and A. D. Wieck, Observation of the Kondo effect in a spin-$\frac{3}{2}$ hole quantum dot, Phys. Rev. Lett. **107**, 076805 (2011).

[58] V. Kumar, Y. Duo, P. See, J. P Griffiths, D. A Ritchie, I. Farrer, and S. Kumar, Data of the research article titled "Correlation effects mediated by disorders in one-dimensional channels" (University College London, Dataset. https://doi.org/10.5522/04/29264993).